size of A ion and the symmetry of NbO_6 on both the crystal symmetry and the property of A ion. The absorption edge decreased, as the basicity of A ion was increased and the size of A ion was decreased. ESR spectra of Cu^{2+} showed nearly isotropic shapes with the exception of SCN and the covalency of Cu-O bond depended on the basity and the size of A ion. The important factors, which affect the bonding character of B-O and the symmetry of BO_6 octahedron, were the size ad the basicity of A ion.

Acknowledgement. This work was financially supported by Korea Science and Engineering Foundation in 1991.

References

1. G. Blasse, *J. Inorg. Nucl. Chem.*, **27**, 993 (1965).
2. E. Takayama-Muromachi and A. Navrotsky, *J. Solid State Chem.*, **72**, 244 (1988).
3. K. Hayashi, H. Noguchi, and M. Ishii, *Mat. Res. Bull.*, **21**, 401 (1986).
4. T. Nakamura and J. H. Choy, *J. Solid State Chem.*, **20**, 233 (1977).
5. R. C. Buchanan, "Ceramic Materials for Electronics", Marcel Dekker, Inc., New York, U.S.A. 1986.
6. P. Ganguly, N. Y. Vasanthacharya, C. N. R. Rao, and P. P. Edwards, *J. Solid State Chem.*, **54**, 400 (1984).
7. B. Jaffe, W. R. Cook Jr., and H. Jaffe, "Piezoelectric Ceramics", Academic Press, London, England, 1971.
8. A. W. Sleight and J. F. Weiher, *J. Phys. Chem. Solids*, **33**, 679 (1972).
9. A. R. West, "Solid State Chemistry and its Applications", John Wiley & Sons Ltd., New York, U.S.A. 1984.
10. R. D. Shannon and C. T. Prewitt, *Acta Cryst.*, **B25**, 925 (1969).
11. A. Halliyal, U. Kumar, R. E. Newnham, and L. E. Cross, *Am. Ceram. Soc. Bull.*, **66**, 671 (1987).
12. M. Lejeune and J. P. Boilot, *Ceramics International*, **8**, 99 (1982).
13. S. L. Swartz and T. R. Shrout, *Mat. Res. Bull.*, **17**, 1245 (1982).
14. G. Blasse, *J. Inorg. Nucl. Chem.*, **35**, 1347 (1975).
15. G. Shirane, R. Pepinsky, and B. C. Frazer, *Acta Cryst.*, **9** 131 (1956).
16. J. A. Alonso and I. Rasines, *J. Phys. Chem. Solids*, **49**, 385 (1988).
17. F. Galasso, L. Katz, and R. Ward, *J. Am. Chem. Soc.*, **81**, 820 (1959).
18. F. Galasso and W. Darby, *J. Phys. Chem.*, **66**, 131 (1962).
19. N. Ramadass, J. Gopalakrishnan, and M. V. C, Sastri, *J. Inorg. Nucl. Chem.*, **40**, 1453 (1978).
20. J. T. Last, *Phys. Rev.*, **105**, 1740 (1957).
21. A. F. Corsmit, H. E. Hoefdraad, and G. Blasse, *J. Inrong. Nucl. Chem.*, **34**, 3401 (1974).
22. G. Blasse and A. F. Corsmit, *J. Solid State Chem.*, **10**, 39 (1974).
23. E. Husson, L. Abello, and A. Morell, *Mat. Res. Bull.*, **25**, 539 (1990).
24. G. Blasse and A. F. Corsmit, *J. Solid State Chem.*, **6**, 513 (1973).
25. R. E. Coffman, *J. Chem. Phys.*, **48**, 609 (1968).

Infrared Spectra and Electrical Conductivity of The Solid Solutions $X\ MgO+(1-X)\ \alpha-Nb_2O_5$; $0.01 \leq X \leq 0.09$

Zin Park, Jong Sik Park, Dong Hoon Lee, Jong Ho Jun†, Chul Hyun Yo, and Keu Hong Kim*

Department of Chemistry, Yonsei University, Seoul 120-749
†Department of Biochemistry, Kon-Kuk University, Chungju 380. *Received August 10, 1991*

Changes in network structures of α-Nb_2O_5 in the $X\ MgO+(1-X)$ α-Nb_2O_5 solid solutions occurring as the MgO doping level (X) was varied were investigated by means of infrared spectroscopy and X-ray analysis. X-ray diffraction revealed that all the synthesized specimens have the monoclinic structure. The FT-IR spectroscopy showed that the system investigated forms the solid solutions in which Mg^{2+} ions occupy the octahedral sites in parent crystal lattice. Electrical conductivities were measured as a function of temperature from 600 to 1050℃ and P_{O_2} form 1×10^{-5} to 2×10^{-1} atm. The defect structure and conduction mechanism were deduced from the results. The 1/n value in $\sigma \propto P_{O_2}^{1/n}$ is found to be $-1/4$ with single possible defect model. From the activation energy (E_a=1.67-1.73 eV) and the $1/n$ value, electronic conduction mechanism is suggested with a doubly charged oxygen vacancy.

Introduction

The polymorphism of niobium pentoxide has been studied by several investigators. The α form of Nb_2O_5 is the most thermodynamically stable polymorph in the high temperature. The transition temperature of the α form from the low temperature modification has been found to be approximately 830℃ and the transition is irreversible[1]. The structure of α-Nb_2O_5 is derived from the ReO_3-type structure. The crystal structure of α-Nb_2O_5 has been found to be monoclinc, space

group C_2, P_2 with $Z=14$[1-4].

McConnel *et al.*[5] refinded the structure of the α form of Nb_2O_5 and reported that one niobium atom out of 28 occupies a tetrahedral site with the remaining atoms in octahedral sites. The octahedrons arrange regularly to 3×4 blocks and 3×5 blocks, and they are corner-shared each other in both blocks and edge-shared between blocks[3]. Internal vibrations of NbO_6 octahedron were considered from IR and Raman spectra analyses of α-Nb_2O_5. ν_1, ν_2 and ν_5 vibrational modes are Raman active and ν_3 and ν_4 modes are IR active in Oh. Although the NbO_6 octahedra practically are distorted, McConnel *et al.*[5] and Balachandran *et al.*[6] reported that the band at 992 cm^{-1} is due to the ν_1, the band at 650 cm^{-1} is ν_2, and ν_5 mode appears in the region 350-550 cm^{-1} by Raman spectra analyses. Furthermore, Raman band at 850 cm^{-1} shows internal vibrations of NbO_4 tetrahedra. McDevitt *et al.*[7] reported IR broad bands were observed at 300, 480 and 670 cm^{-1} in α-Nb_2O_5.

It has been reported that α-Nb_2O_5 is a nonstoichiometric oxide showing oxygen-deficient by departure of oxygen from stoiochiometry since Brauer[8] found that α-Nb_2O_5 could exist as a single phase with departure of oxygen from stiochiometry up to $Nb_2O_{4.8}$. Nonstoichiometry of α-Nb_2O_5 was studied by many researchers[9-12]. Kofstad and Anderson[9] found that the relative weight change in α-Nb_2O_5 is proportional to $P_{O_2}^{-1/6}$ at constant temperature over an oxygen pressure range of 10^{-7} to 10^{-18} atm and temperature range of 900 to 1400℃. They concluded that the defect structure in this range of oxygen pressure involves doubly ionized oxygen vacancies.

Balanchandran *et al.*[12] found that the relative weight change is proportional to $P_{O_2}^{-1/6}$ for $P_{O_2}<10^{-12}$ atm and temperature range of 950 to 1250℃ but for higher P_{O_2} values, the relative weight change becomes almost independant of P_{O_2}. They reported that these results show that for lower P_{O_2} ranges, doubly ionized oxygen vacancies are major defect structure, but for higher P_{O_2} ranges, doubly charged acceptor impurities are major defect structures. The fact that the oxygen partial pressure dependence of the electrical conductivity changes from −1/6th to −1/4th power as P_{O_2} is increased has been interpreted in terms of doubly and singly ionized oxygen vacancies and acceptor impurities[13]. Kling[14] measured the electrical conductivity of α-Nb_2O_5 as function of P_{O_2}, and reported an increase in conductivity with a decrease in P_{O_2}, characteristic of *n*-type conduction.

Greener *et al.*[15] reported that under a constant ambient oxygen pressure in the temperature range of 300 to 900℃, the isothermal conductivity in the oxygen pressure range 1 to 1×10^{-3} atm was found to be proportional to $P_{O_2}^{-1/4}$ with an activation energy of 1.65 eV. The electrical conductivity measurements carried out in mixtures of CO and CO_2 by Kofstad[16] showed −1/6th power dependence for conductivity on P_{O_2} in the temperature range from 750 to 1100℃. The ionic transport number in α-Nb_2O_5 is found to be less than 0.05 by Elo *et al.*[17]. Yahia[4] calculated the electronic mobility in α-Nb_2O_5 at 900℃ as $7\times10^{-2}\cdot cm^{-2}\cdot V^{-1}sec^{-1}$.

As mentioned above, the electrical conductivity for α-Nb_2O_5 was studied by several investigators, however, the electrical conductivity and defect structure for cation-doped α-Nb_2O_5 systems have not been studied. Thus in the present work, we will present the result of electrical conduction mechanism and possible defect structure of α-Nb_2O_5 doped with MgO as a function of temperature and oxygen partial pressure.

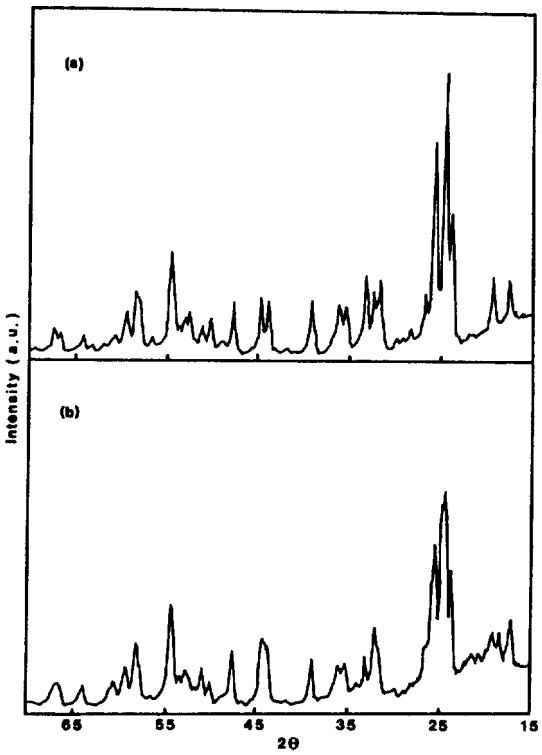

Figure 1. X-ray diffraction patterns of pure α-Nb_2O_5 (a) and 9 mol% MgO-doped α-Nb_2O_5 (b) systems.

Experimental

The pure Nb_2O_5 (99.99%, Fluka Chemie AG Co.) and MgO (99.99%, Fluka Chemie AG Co.) powders were weighed to produce Nb_2O_5 doped with 1, 3, 5, 7 and 9 mol% of MgO and were ground and mixed on agate mortar for several hours, stirred for an additional 24 hr in ethyl alcohol, calcined at 700℃ for 18 hr in air to eliminate CO_2, H_2O, etc. The powders were made into pellets under a pressure of 49 MPa and sintered at 1350℃ for 36 hrs and quenched to room temperature. The specimens were cut into a rectangular shape, 1.0×0.4×0.11 cm^3 in size, and four equally spaced holes were drilled in a row on one face to provide a four-probe contact.

Changes in network structure of α-Nb_2O_5 in the X MgO+$(1-X)$ α-Nb_2O_5 solid solutions occurring as the MgO doping is varied were investigated by IR spectroscopy (Digilap-Division, FTS-80) and X-ray diffraction (Philips PW1710, CuKα) which revealed that all the synthesized specimens have the monoclinic structure. The FT-IR spectroscopy showed that the number of bands decreases with increasing amount of MgO. XRD patterns for pure and 9 mol% MgO-doped α-Nb_2O_5 are shown in Figure 1. The thermogravimetry and differential scanning calorimetry (Rigaku PTC-10A) measurements were performed to investigate any change of nonstoichiometry and phase transition. The results of these measurements showed that there was no phase transition and their results are shown in Figure 2.

The electrical conductivity was measured according to Val-

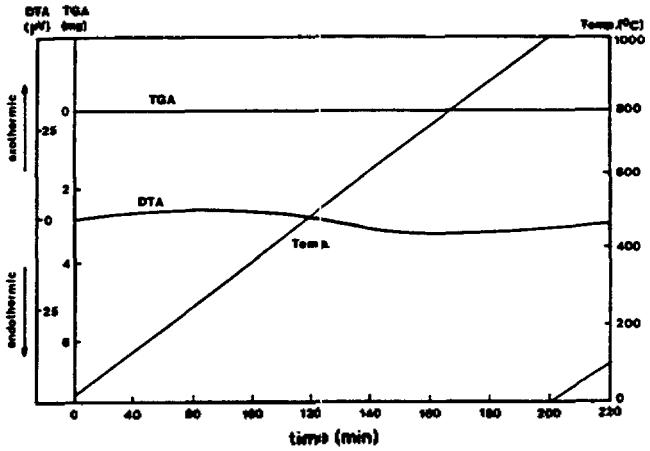

Figure 2. DTA and TGA of 5 mol% MgO-doped α-Nb_2O_5 system.

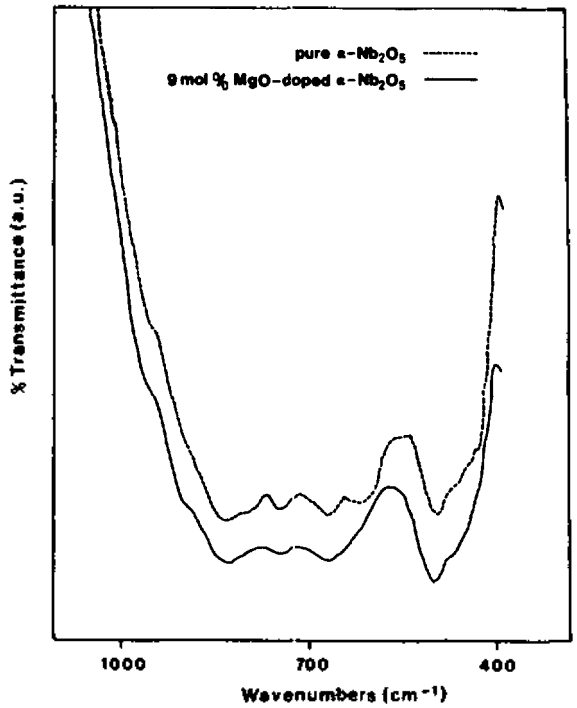

Figure 3. IR spectra of pure α-Nb_2O_5 and 9 mol% MgO-doped α-Nb_2O_5 systems.

des' technique[18]. The potential difference was measured by a Leed & Northrup 7555 K-5 type digital multimeter, and the current through the sample was measured by a Keithley 610C digital electrometer.

The current through the sample was maintained between 10^{-8} and 10^{-2} A by a rheostat and potential across the two inner probes was maintained less than 0.8 V. The electrical conductivity was measured in the 600~1050℃ temperature range under oxygen partial pressure from 1×10^{-5} to 2×10^{-1} atm.

Results and Discussion

IR Spectra. In niobium pentoxide systems, the binding

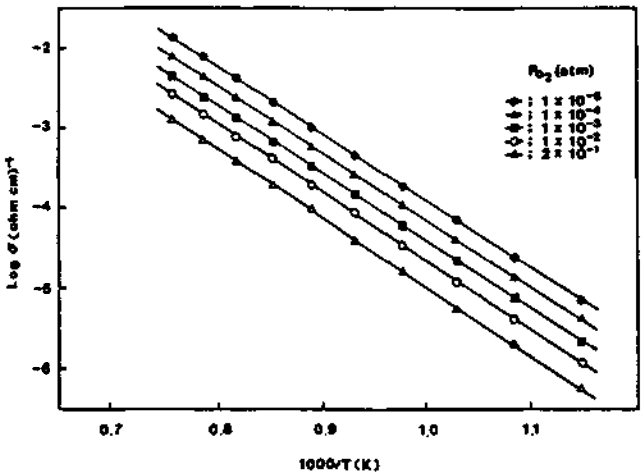

Figure 4. Temperature dependence of electrical conductivity of 5 mol% MgO-doped α-Nb_2O_5 system at constant oxygen partial pressure.

forces within the metal-oxygen octahedra are large compared to the crystal binding forces[5]. Thus the internal vibrations of the NbO_6 group in the solid should be quite close to the free-ion modes, the external modes occurring at considerably lower frequencies, usually below 200 cm^{-1}, than the internal modes. Although strict factor group analysis is difficult in this system, we can fruitfully interpret the IR spectra with the internal mode approach in terms of discrete metal-oxygen polyhedra since defect-induced one-phonon absorptions[19] due to many oxygen deficiencies give rise to local modes.

IR spectra of pure α-Nb_2O_5 and 9 mol% MgO-doped α-Nb_2O_5 system are shown in Figure 3. There are more eight IR bands observed in pure α-Nb_2O_5 and the number of bands decreases with increasing amount of MgO. The structure of pure α-Nb_2O_5 has two kinds of metal atom sites; tetrahedral site and octahedral site, and each site takes two IR active modes. Two T_2 modes induced from the tetrahedral site are asymmetric stretching (ν_3^T) and asymmetric bending (ν_4^T). Vibrations of octahedral site lead to two T_{1u} modes, asymmetric bending (ν_3^O) and out-of-plane bending (ν_4^O). The metal ion in Td site, though its population is only one twenty-eighth, is so distorted[3] that its intensity is expected to be strong. On the other hand, octahedrons are connected by corner-sharing in both blocks and by edge-sharing between blocks, so that the peaks due to octahedral sites are considered to be asymmetric or splitted. Based on these analyses, 500 cm^{-1} peak can be assigned to ν_4^T, 750 cm^{-1} peak to ν_3^T, 670 and 615 cm^{-1} peaks to ν_4^O, and 835 cm^{-1} peak and shoulder at 795 cm^{-1} to ν_3^O, respectively.

When 9 mol% MgO is doped into α-Nb_2O_5, two peaks (ν_4^O) at 670 and 615 cm^{-1} are changed to one peak at 660 cm^{-1}, a peak at 835 cm^{-1} and a shoulder at 795 cm^{-1} are sharpened at 820 cm^{-1}, and very broad band at 445 cm^{-1}[17] due to MgO does not appear. This result implies that the Mg^{2+} ions occupy the octahedral sites in the parent structure and cause the reduction of distortion in octahedrons, confirming the solid solution.

Conductivity. The temperature dependence of the electrical conductivity for the 5 mol% MgO-doped α-Nb_2O_5 system is shown in Figure 4. The activation energy can be taken

Table 1. Activation Energies for MgO-Doped α-Nb_2O_5 Systems

Dopping MgO mol%	Po_2(atm) 2×10^{-1}	1×10^{-2}	1×10^{-3}	1×10^{-4}	1×10^{-5}
	(eV)				
1	1.69	1.68	1.67	1.70	1.69
3	1.72	1.73	1.69	1.72	1.71
5	1.73	1.71	1.69	1.67	1.70
7	1.71	1.69	1.71	1.69	1.70
9	1.69	1.73	1.70	1.70	1.69

Table 2. Po_2 Dependence of Electrical Conductivity in MgO-Doped α-Nb_2O_5 Systems

Dopping MgO mol%	T(℃)	600	700	800	900	1000	1050
				(n)			
1		4.18	4.09	4.09	4.00	4.01	4.15
3		4.19	4.00	3.97	4.00	4.05	4.10
5		4.05	4.09	3.95	4.01	4.03	4.10
7		4.10	4.18	4.07	3.90	4.10	4.15
9		4.00	4.21	4.05	4.05	3.97	4.05

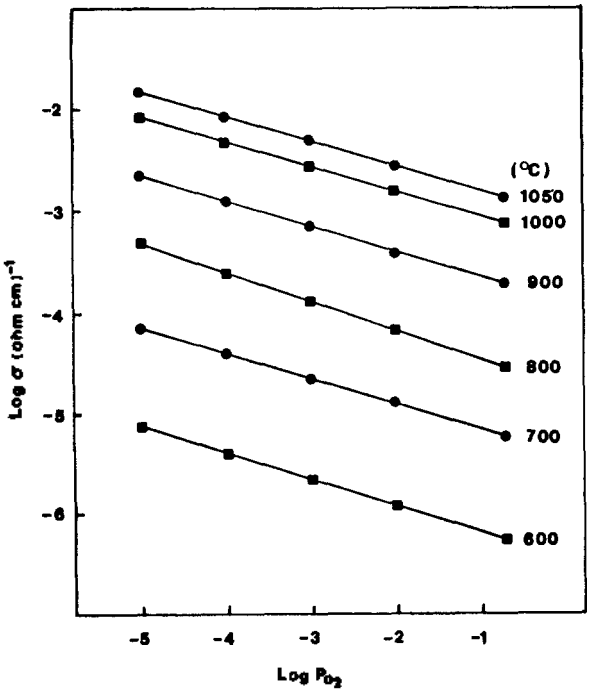

Figure 5. Isothermal electrical conductivity as a function of oxygen partial pressure for a 5 mol% MgO-doped α-Nb_2O_5 system.

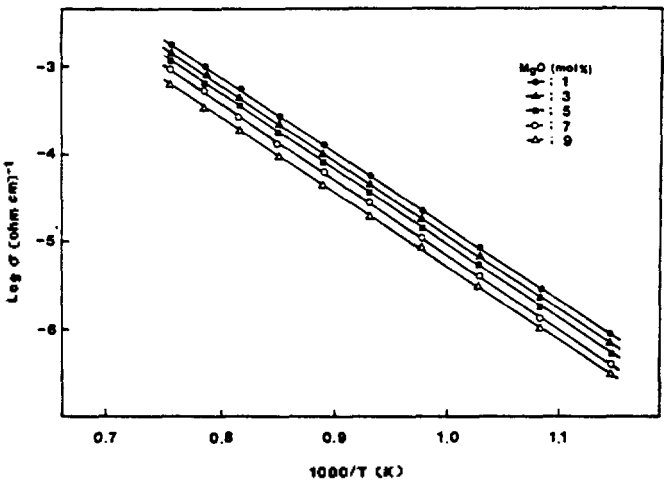

Figure 6. Temperature dependence of electrical conductivity of various MgO-doped α-Nb_2O_5 systems under Po_2=0.2 atm.

from the slope of Figure 4. From these data, the slopes are constant in this experimental temperature range. The activation energies for each sample taken from the Arrhenius equation are listed in Table 1. As can be seen in Table 1, the activation energy for each sample is almost the same. So, the conduction mechanism of the solid solution is expected to be same.

The electrical conductivity of 5 mol% MgO-doped α-Nb_2O_5 system in the temperature range 600 to 1050℃ and in equilibrium with oxygen partial pressures between 10^{-5} and 0.2 atm is shown in Figure 5. The oxygen partial pressure dependence of electrical conductivity for each sample is listed in Table 2. The results show that the conductivites of all solid solutions are proportional to the −1/4th power of oxygen partial pressure in all experimental conditions. This linearity affords an opportunity to determine the defect model responsible for the n-type electrical conductivity in these samples. The variation of the electrical conductivity with the oxygen partial pressure is calculated in terms of the oxygen vacancy defect model.

The equilibrium in extrinsic conduction for defect model is

$$2MgO \overset{K_1}{\rightleftarrows} 2Mg'''_{Nb} + 2O_O + 3V_O^{\cdot\cdot} \quad (1)$$

The equilibrium in intrinsic conduction is

$$O_O \overset{K_2}{\rightleftarrows} 1/2O_2 + V_O^{\cdot\cdot} + 2e' \quad (2)$$

Since the conduction is the sum of intrinsic and extrinsic contributions, the total conduction can be represented as combining equilibria (1) and (2) as follows;

$$2MgO \overset{K_3}{\rightleftarrows} 2Mg'''_{Nb} + 5V_O^{\cdot\cdot} + 4e' + O_2 \quad (3)$$

If the law of mass action is applied to equilibrium (1)

$$[V_O^{\cdot\cdot}] = 3/2[Mg'''_{Nb}] = \text{const.} \quad (4)$$

Then the oxygen vacancy concentration is determined by the impurity content. The equilibrium constant of Eq. (3) is

$$K_3 = [Mg'''_{Nb}]^2 \cdot [V_O^{\cdot\cdot}]^5 \cdot n^4 \cdot Po_2 \quad (5)$$

where $[e']=n$. Substituting Eq. (4) into Eq. (5), the result for the electron concentration is

$$n = K' \cdot Po_2^{-1/4} \quad (6)$$

where $K' = [2/3]^{5/4} \cdot [Mg'''_{Nb}]^{-7/4} \cdot K_3^{1/4}$. On the other hand, since $\sigma = ne\mu$ where μ is the mobility which is independent of Po_2 and e is the charge, the electrical conductivity is proportional

to charge carrier, n.

$$\sigma \propto P_{O_2}^{-1/4} \quad (7)$$

The calculated exponent $-1/4$ based on the $V_{\ddot{O}}$ and electron model is consistent with the experimental value. It is suggested that the possible defect in MgO-doped α-Nb_2O_5 systems be $V_{\ddot{O}}$ and the electrical conduction occur through migration of electron. The fact that the electrical conductivity decreases with increasing mol% of MgO, as shown in Figure 6 means that the doubly ionized oxygen vacancy formed in equilibrium (1) moves the equilibrium (2) toward left-hand side. Therefore, MgO doping reduces the charge carrier concentration and so electrical conductivity.

Acknowledgement. The Present Studies were Supported by the Basic Science Research Institute program, Ministry of Education, 1989.

References

1. F. Holtzberg, A. Reisman, M. Berry, and M. Berkenbilt, *J. Amer. Chem. Soc.*, **79**, 2039 (1957).
2. L. K. Frevel and H. N. Rinn, *Anal. Chem.*, **27**, 1329 (1955).
3. B. M. Gatehouse and A. D. Wadsley, *Acta Cryst.*, **17**, 1545 (1964).
4. J. Yahia, *J. Chem. Phys. Solids*, **25**, 881 (1964).
5. A. A. McConnel, J. S. Anderson, and C. N. R. Rao, *Spectrochim. Acta*, **324**, 1067 (1976).
6. U. Balachandran and N. G. Eror, *J. Mater. Sci. Lett.*, **1**(9), 374 (1982).
7. N. T. McDevitt and W. L. Baun, *Spectrochim Acta*, **20**, 799 (1964).
8. G. Brauer, *Z. Anorg. Allem. Chem.*, **248**, 1 (1941).
9. P. Kofstad and P. B. Anderson, *J. Phys. Chem. Solids*, **21**, 280 (1961).
10. R. N. Blumenthal, J. B. Moser, and D. H. Whitmore, *J. Am. Ceram. Soc*, **48**, 617 (1965).
11. H. Schäfer, D. Bergner, and R. Gruehn, *Z. Anorg. Allgem. Chem.*, **365**, 31 (1969).
12. U. Balanchandran and N. G. Eror, *J. Mater. Sci.*, **17**, 1286 (1982).
13. P. Kofstad, "*Nonstoichiometry, Diffusion and Electrical Conductivity in Binary Metal Oxides*", Wiley-Interscience, New York, 1972, p. 188.
14. H. Kling, "*The Technology of Columbium*", John Wiley & Sons, New York, 1958, p. 87.
15. E. H. Greener, D. H. Whitmore, and M. E. Fine, *J. Chem. Phys.*, **34**, 1017 (1961).
16. P. Kofstad, *J. Chem. Phys.*, **23**, 1571 (1962).
17. R. Elo, R. A. Swalin, and W. K. Chen, *J. Chem. Phys. Solids*, **28**, 1625 (1967).
18. L. B. Valdes, *Proc. IRE*, **42**, 420 (1954).
19. J. T. Houghton and S. D. Smith, "*Infra-Red Physics*", Oxford University Press, G. B., 1966, p. 108.

Substitution Effect of Fluorine on $HoBa_2Cu_3O_{7-x}F_y$ ($0.0 \leq y \leq 0.5$) Superconductors

Jong Sik Park, Seong Han Kim, Hong Seok Kim, Seung Koo Cho, and Keu Hong Kim*

Department of Chemistry, Yonsei University, Seoul 120-749. Received August 16, 1991

High-Tc superconducting materials, $HoBa_2Cu_3O_{7-x}F_y$ with $0.0 \leq y \leq 0.5$, were synthesized by ceramic method and studied by X-ray diffraction, thermogravimetric analysis, differential thermal analysis, scanning electron microscopy and resistivity measurement. From the X-ray diffraction data, it was found that the samples had only single phase of which lattice volumes were decreased in proportional to the amount of fluorine, which indicated that the relatively small fluorine atoms are effectively substituted for the oxygen sites. Also, an anomalous phenomenon appeared that the peak intensites of (001) planes were greatly increased as fluorine contents increased. SEM photographs revealed that the grain sizes were enlarged progressively with fluorine contents. This fact could be explained along with DTA & TGA data that the incoporation of fluorine gave rise to lowering the melting point. Tc decreased as the incorporation of fluorine content increased. This implies that the superconducting electrons are perturbed due to the substitution of electronegative fluorine atom.

Introduction

Since the discovery of $YBa_2Cu_3O_{7-x}$ (YBCO) superconductor[1] with Tc more than 90 K, lots of experiments[2-5] were carried out to search for the doping effect of the impurity-substituted YBCO superconductors. Based on these experimental results, the doping effect of impurities on superconductivity and structural changes induced from substitutions are helpful to lighten the high-Tc superconducting mechanism which is not well known yet.

Baetzold[6] peported that when the ferromagnetic rare-earth metal ions such that La^{3+}, Nd^{3+}, Eu^{3+}, Gd^{3+}, Ho^{3+}, Er^{3+} and Lu^{3+} were substituted for Y^{3+} sites of YBCO, no dramatic changes in physical properties could occur. Ho *et al.*[7] explained from these results that there were no interactions between spins of the ferromagnetic elements substituted in